Biochimica et Biophysica Acta, 1056 (1991) 149–158

ADONIS 000527289100052U

BBABIO 43319

On the action spectrum of the photoelectric transients of bacteriorhodopsin in solid-state films

Alan R. McIntosh and François Boucher

Centre de recherche en photobiophysique, Université du Québec à Trois-Rivières, Trois-Rivières (Canada)

(Received 2 April 1990)

Key words: Bacteriorhodopsin; Purple membrane; Action spectrum; Photoelectric effect; Charge displacement currents

We have measured the time-resolved charge displacement currents of bacteriorhodopsin (BR) from *Halobacterium halobium* in multilayer arrays of well-oriented purple membranes in photoelectric cells with the sandwich electrode configuration: SnO_2 | BR | Ag. The purple membrane cells were irradiated by dye laser pulses entering the cells through the light-transmitting SnO_2 electrode. The photochemical cycle of BR was found to be reversible in these solid films, and we observed a major decay component for the M intermediate with a decay time of 46 ± 3 ms as measured by the transient optical absorption at 412 nm. We also observed a minor component ($\leqslant 5\%$ of the total amplitude) with a decay time of 0.97 ± 0.15 s. We measured the early action spectrum for the instrument limited amplitudes of the photoelectric behaviour: this action spectrum differed from the absorption spectrum of the absorbing BR pigment. However, the action spectrum measured 500 μs after flash excitation was in agreement with the absorption spectrum of BR. We attribute the nature of the early action spectrum to the presence of red and blue absorbing species which are not capable of pumping protons across the purple membrane bilayer. We also measured the charge displacement currents when the purple membrane cells were perturbed by small applied voltages with a specific polarity: for conduction of negative charges in the same direction as vectorial proton transport, enhanced transient photocurrents resulted. We interpret these enhanced photocurrents in terms of an enhancement of observed charge separation resulting from a reduced back reaction from the K intermediate of the photocycle.

Introduction

Bacteriorhodopsin is the only protein isolated from the purple membrane fraction of *Halobacterium halobium* [1], and it possesses a photochemical cycle with the classic intermediates K, L, M, N and O which can be monitored by absorption spectroscopy from nanoseconds to seconds [2]. The molecular architecture of this proton pump has been the subject of recent biophysical investigations, including the measurement of the orientation of the plane of the retinylidene chromophore relative to the purple membrane plane [3,4]. One recent model [4] for the movement of charges in the BR photochemical cycle places the orientation of the N–H bond towards the exterior of the membrane, based on linear dichroism results, although an opposite orientation has been assigned in another model [5]. In both of these models, the Schiff base of BR is hydrogen-bonded to its counterion, probably Asp-212. Upon photoisomerization from the 13-*trans* to 13-*cis* forms of the chromophore, the Schiff base is carried away from the proximity of Asp-212 and Tyr-185. In the K and L intermediates, the Schiff base is probably hydrogen bonded to Asp-85; and in the L to M transition, the Schiff base proton is transferred to Asp-85. In the C-T model [6], an isomerization-induced conformational change (T to C) permits the reprotonation of the Schiff base by a residue other than Asp-85 so that proton pumping from the cytoplasm to the exterior of the membrane is the final result.

It is clear that the primary photochemistry and subsequent events involve the creation of dipoles and the movement of individual charges. These two kinds of charge displacements have been detected together, but not resolved, in various samples of oriented purple membrane patches in aqueous suspensions [7,8], at interfaces [9,10], and also in a number of solid state

Abbreviation: BR, bacteriorhodopsin.

Correspondence: A.R. McIntosh, Centre de recherche en photobiophysique, Université du Québec à Trois-Rivières, Trois-Rivières, Québec, Canada, G9A 5H7.

systems: formed by electrodeposition [11–18], by incorporation in polyacrylamide gels [19,20], and by a Langmuir-Blodgett protocol [21]. However, the molecular details giving rise to the photocurrents remain to be elucidated, including the question of separating the contribution of dipole creation from that of charge migration. It is known from the photochemistry of rhodopsin that the early charge separation plays a role in the storage of photochemical energy [22,23]. In addition, optical second-harmonic generation [3] and spectroscopic [24] measurements point towards a mechanism in which the protonated Schiff base in bacteriorhodopsin is separated from a negative counter ion, probably Asp-212, during the primary photoisomerization.

By an analysis of purple membranes as displacement current generators, Keszthelyi's group [7] first proposed that protons undergo a slingshot type of mechanism in which they first recoil then advance in the direction of vectorial proton transport. The same group also showed [8] that the displacement current with a negative phase, relative to the proton pumping, is associated with the charge displacement events of the primary photochemistry resulting in the K intermediate. Indeed, all oriented BR samples are characterized by the distinctive bipolar character of the charge displacement currents which is common to oriented BR membrane systems [7–21]. However, another important consideration [3,15] is that changes in electronic charge density of the retinylidene chromophore occur at the same time as the photoisomerization; and the electronic charge distribution also should influence the protein's structural alterations.

The object of the present study was twofold: (1) to characterize the integrity of the photochemical cycle in these solid state films which are dehydrated relative to aqueous suspensions and (2) to examine the early events of the charge displacement currents on a microsecond timescale to examine the photochemical mechanism of dipole splitting and subsequent charge migration. We adopted a first approach to these questions by measuring the action spectra of the charge displacement currents in solid films in the early 1–500 μs time domain. Previous action spectra have only been measured for hydrated membranes [10] or have only been measured under steady-state conditions [18,20,21] and thus lacked any detailed kinetic information. We chose to use multilayers of purple membranes because they can be perfectly oriented by an electrodeposition technique [11], and they give well resolved charge displacement currents in the time domain. One further advantage of measuring charge displacement currents in the solid state is that there is no ambiguity concerning proton migration at and beyond the aqueous interface [7]. For instance, voltage clamp measurements [25] have demonstrated the possibility of two components for the displacement currents: an oriented dipole mechanism and interfacial charge transport. Thus, in aqueous systems, it is essential that the bilayer aqueous interfaces be characterized in order to interpret the kinetics of the photochemical charge displacements, including any back-reactions [25,26]. In the solid-state multilayer system, there is essentially no interfacial charge transport and the samples are still reversibly active [13]; but the question of the photochemical efficiency in these dehydrated solid films remains unanswered to this day. With regard to reversibility, we report some optical measurements which show that the photochemical cycle of BR in this solid-state system is slower, but that it can still be reversibly cycled.

Materials and Methods

Purple membranes were isolated from the S-9 strain of *Halobacterium halobium* according to established methods [27]. Prior to electrodeposition, the purple membranes were resuspended and centrifuged three times in deionized and quartz-distilled water so that the conductivity was less than 0.1 μS/cm. A template was used to shape the SnO_2 electrode to the desired form on standard 25×75 mm glass slides, and the SnO_2 was deposited by reactive sputtering in an Edwards vacuum sputtering system with 10% oxygen and the balance argon at a total pressure of 10^{-3} torr. The purple membranes were electrodeposited on these SnO_2 electrodes by applying an electric field of about 30 V/cm across a 3 mm cell to achieve the orientation, electrophoresis, and deposition of the purple membrane fragments (usually in less than ten seconds) on the optically transmitting SnO_2 electrodes on glass slides [11]. We performed electrical measurements on these dried solid films which had absorbances between 0.1 and 1.0 at 568 nm for light-adapted slides at 50% relative humidity. On certain slides with absorbances less than 0.3, we were able to measure the thickness of the purple membrane multilayers at a relative humidity of 50% using a Varian Model 980-4000 interferometric microscope (with a Fizeau plate). These measurements provided a calibration of (5600 ± 400) Å for an absorbance of 0.1 at 568 nm for electrodeposited light-adapted purple membrane fragments: this calibration has not been reported previously to the best of our knowledge. This measurement permits an estimate of the extinction coefficient for solid films of electrodeposited purple membranes: $\alpha = (1.79 \pm 0.13) \cdot 10^3\ \mathrm{cm}^{-1}$.

For electrical measurements, a second silver electrode was evaporated in vacuo on top of the purple membranes so as to achieve the sandwich geometry, SnO_2 | BR | Ag. All measurements of the electrical activity were performed at a relative humidity of 50% which was maintained by equilibration with a saturated calcium nitrate solution at 25 °C in a closed box. The

electrodes were connected to the high impedance input of an operational amplifier in a current-integrating circuit which stored the integrated charges on a 0.5 nF capacitor and produced a voltage at the output which was proportional to these stored charges. Upon electrical connection to a thin film sample, the amplifier circuit had a rise time of approx. 1.5 μs and an RC time constant of 11 ms for holding the integrated charges. The RC time constant of the thin film must have caused some distortion of the time profile of the photoelectric transients. However, the time constant of the photoelectric response under open circuit conditions was similar to those of other thin film bacteriorhodopsin membrane electrodes [11], but we did not use shunting resistances which could affect the photoelectric signals due to changes in the effective RC time constants. We did observe significant changes in the time profiles when various shunting resistances were employed, and we chose to avoid this difficulty. Finally, an integrating amplifier was used for these measurements so as to avoid problems with oscillating feedback responses at the input of the operational amplifier which were usually present in the current/voltage conversion mode of amplification for thin film photocells due to their intrinsically small electrical capacitance values (see later). We acknowledge that much faster time responses can be obtained by using current/voltage conversion amplifiers for thicker aqueous cells with much larger electrical capacitance values [19], but the requirement of homogeneous light absorption prevented us from substantially increasing the solid film thicknesses in the cells of this work.

The sandwich cells were excited through the light-transmitting SnO_2 side of the cells by laser pulses at 0.2 Hz with a full width at half-maximum (FWHM) of 0.6 ns from a Photochemical Research Associates (PRA) LN102 dye laser which was pumped by a PRA LN1000 nitrogen laser. By selecting suitable dyes, we able to produce light pulses from the dye laser between 470 nm and 700 nm (at 2 nm intervals) which gave saturating electrical responses at light energy levels of approx. 100 μJ for purple membrane samples with a 0.3 absorbance. When we measured the action spectra for these samples, we were careful to diffuse the dye laser beam so that the measured amplitudes always responded linearly with the energy input of about 1–20 μJ as measured by a Gentech ED-100 thermoelectric light pulse energy meter at each wavelength. It should be noted that the laser light was unpolarized at the sample position after passage through a diffusing lens and frosted glass plate. Each action spectrum was calculated in terms of the number of photons incident on the purple membrane multilayers by correcting for a small absorption by the SnO_2 electrode at all wavelengths. In fact, the silver electrode acted as a mirror for these visible light pulses so that the incident photons traversed the purple membrane multilayer two times, but we deemed multiple internal reflections to be of minor importance from a consideration of the Fresnel coefficients for internal reflections, assuming a refractive index of 2.0 for SnO_2 and 1.5 for the purple membranes.

By assuming an idealized equivalent circuit with a resistance and capacitor in parallel for the sandwich cells, we estimated the circuit element values at 50% relative humidity using a standard a.c. impedance technique with frequencies between 0.005 Hz and 100 Hz. The calculated resistance was usually between 50 and 200 MΩ for samples with absorbances between 0.3 and 1.0, and this value was strongly influenced by the water content of the samples. However, the capacitance was usually between 0.5 nF and 1 nF, which agreed with the order of magnitude estimate of the geometric capacitance calculated by assuming a dielectric constant between 3 and 8 for the membranes. (The active area of the purple membrane sandwich cell was approx. 0.45 cm^2, and the thickness was typically 1–3 μm.) On application of small (up to ± 50 mV) voltages to well behaved cells, there was no evidence for any significant rectifying behaviour in these cells when we inspected the current–voltage curves over the frequency range from 0.005 Hz to 100 Hz.

Some cells with the least noise in their current–voltage curves were chosen for the experiment in which we measured the charge displacement currents while applying d.c. voltages of 20 mV to 100 mV across the cells. According to the measured 100 MΩ internal resistances, these applied voltages should have resulted in d.c. currents of about 1 nA. We were able to measure some of these d.c. currents in the range of 0.1 to 1.0 nA, using a Keithley Model 616 digital electrometer. Since we were using polarizable electrodes in this work, d.c. currents in the range below 1 nA indicate a small leakage between the electrodes as compared with the much larger microampère transient photocurrents. Furthermore, the current/voltage plots of the impedance measurements showed some current fluctuations for most samples, indicating that the leakage currents were variable.

In the steady-state absorption spectra, all solid oriented films were measured at an angle of incidence of 90°, and under these conditions, we were unable to detect any dichroic absorption in these samples using polarizing filters. We also carried out some time-resolved ΔA optical measurements on the immobilized and oriented BR films on SnO_2 slides using a JK Lasers System 2000 Nd-YAG laser with a FWHM of 20 ns at 532 nm, and a xenon arc lamp was used as a monitoring beam in conjunction with a 412 nm interference filter. The analyzing beam was incident at an angle of 45° to the film, and the observed ΔA values were independent of the angle of incidence between 40° and 50°. The detector was a Hamamatsu S1722-01 photodiode with an amplifier which had a time response of about 100 ns.

The laser pulse was diffused so that no more than 1 mJ at 532 nm was incident on the purple membrane samples. Finally, the detector was sufficiently removed from the sample to minimize the collection of scattered light from the monitoring beam.

Results and Discussion

From previous measurements [13] of the permanent electric dipoles of purple membrane fragments at pH 7 in aqueous suspensions, it has been determined that protons move in the direction of the positive charge of the purple membrane's permanent electric dipole. As the purple membranes were electrodeposited on an SnO_2 anode, this implies that the direction of pumping of protons in these oriented multilayers is towards the silver electrode as shown in Fig. 1a. In Fig. 1b, the early version [28] of the photochemical cycle of BR shows the major optical intermediates involved in the operation of the proton pump. Subsequent versions of the photochemical cycle contain branching pathways including light- and dark-adapted cycles [2], but the main features of the original version are intact in more recent updates of the photochemical cycle [29].

Optical measurements

In Fig. 2, we compare the absorption spectrum of an aqueous suspension of purple membranes at pH7 with that of an electrodeposited multilayer film on SnO_2. Both preparations of purple membranes were light adapted, and we observed $\lambda_{max} = 568$ nm in both cases. There should be a sensitivity of the absorption spectra of BR [28] to dark adaptation forming BR^{558} (with $\lambda_{max} = 558$ nm) and to light adaptation forming BR^{568} (with $\lambda_{max} = 568$ nm) which we also observed in our oriented multilayer films of purple membranes (not shown). We note that there are some differences in the spectra of the solid films relative to that of aqueous suspensions, particularly the existence of the broad red shoulder on the the solid film spectrum of Fig. 2. The spectrum of the solid oriented film was corrected for any absorption by the SnO_2 electrode, however there was some residual SnO_2 absorbance caused by changes in the SnO_2 electrode following electrodeposition in the region of $\lambda < 400$ nm (not shown in Fig. 2). In addition, the red shoulder of the solid film spectrum was enhanced for samples which were electrodeposited for periods of time longer than 10 s. The spectrum of the oriented film of Fig. 2 was obtained for a sample which was electrodeposited for 15 s, and shorter electrodeposition times resulted in samples with spectra having weaker absorbances in the red (e.g., see Fig. 4).

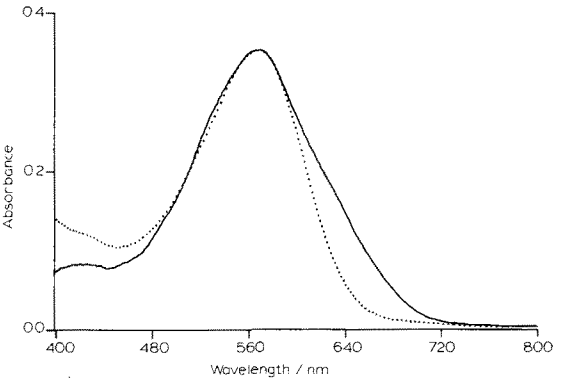

Fig. 2. Typical absorption spectrum of a purple membrane suspension in deionized water at pH 7 at 298 K (dotted line); typical absorption spectrum of electrodeposited purple membranes oriented on SnO_2 at 298 K (solid line).

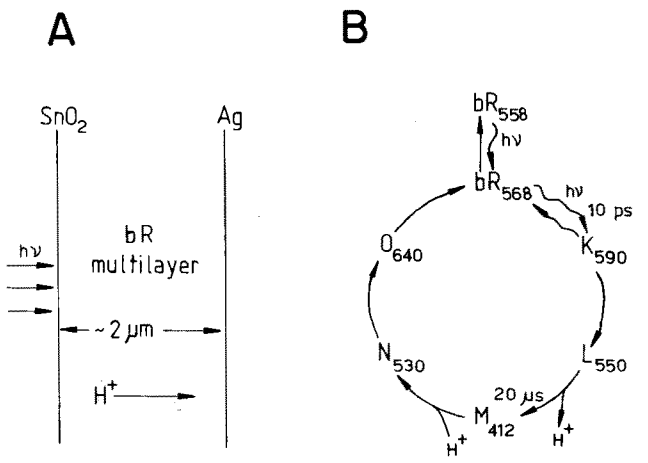

Fig. 1. (A) Schematic view of a sandwich cell with the vectorial direction shown for proton pumping relative to the external SnO_2 and Ag electrodes; (B) the photochemical cycle of bacteriorhodopsin according to Ref. 28.

We made some measurements of the transient optical absorption of the intermediate M (or M^{412}) at 412 nm which we refer to as ΔA_{412}. We found that the decay of ΔA_{412} was approximately exponential with a decay time of 46 ± 3 ms (see Fig. 3a), slower than the usual 20 ms [19] observed for purple membrane fragments in aqueous suspensions. However, there was an additional small fraction (approx. 2–5%) of the amplitude of ΔA_{412} which decayed with a time constant of 0.97 ± 0.15 s. This slow decay component was also enhanced for samples with long times of electrodeposition. We note Kononenko et al. [17] detected much longer lifetimes for the decay of M^{412} in their electrodeposited samples, but the latter's electrodeposition times (30–240 s) were much longer than those of this work (15 s maximum); and the prolonged applied currents probably affected the former samples.

On comparing the absorption spectra of Fig. 2, the similar bandwidths and absorption maxima suggest that the molar extinction coefficients for the two systems could be similar. However, a careful comparison of extinction coefficients would require a molar concentration measurement of the solid film so that the molar

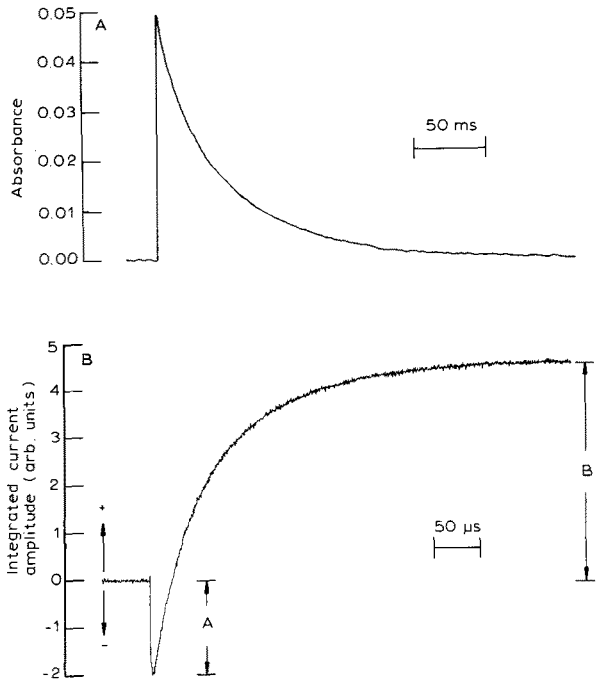

Fig. 3. (A) Typical time-resolved optical absorption measured at 412 nm in a solid state cell with electrodeposited purple membranes at 298 K with an optical absorbance of $A_{568} = 0.5$, excitation at 532 nm with one saturating 1 mJ laser flash. (B) Typical time-resolved integrated displacement current obtained by averaging with 16 dye laser flashes (each with approx. 50 μJ at 570 nm) with excitation through the transparent SnO_2 electrode for a sample with $A_{568} = 0.3$ at 298 K.

extinction coefficient (units of 1 $mol^{-1} \cdot cm^{-1}$) of heterogeneous aqueous suspensions could be related to the absorption coefficient, α (units of cm^{-1}), for homogeneous absorption in the solid films. In the absence of this molar concentration estimate, we shall simply assume that the extinction coefficients for the two systems are similar based on the similar absorption spectra. Empirically, we found that flash induced changes in optical density (ΔA) for electrodeposited samples maintained at 50% relative humidity were comparable to the ΔA values (approx. 0.05) from equal absorbances (approx. 0.5) of purple membranes in aqueous suspensions [28]. Assuming comparable extinction coefficients for the hydrated and dehydrated membrane systems, we conclude that there was only a small ($\leqslant 5\%$) deactivation of BR in our electrodeposited thin films relative to aqueous suspensions. Therefore, the photochemical cycle was slowed down (recycling of M^{412} to BR^{568}), but it appeared to be reversibly cycled upon repetitive excitation of our solid state films at 0.2 Hz. We will return to this important question.

Action spectra of the photocurrents

A typical charge displacement photocurrent measured for our sandwich cells is shown in Fig. 3b, where the measured time dependent voltage is proportional to the integrated charge displacement currents. We will

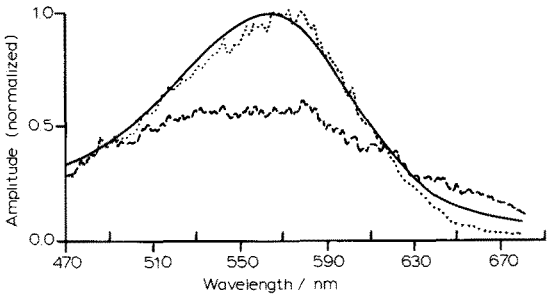

Fig. 4. Absorption spectrum of light-adapted BR multilayers on a SnO_2 electrode (corrected for SnO_2 absorption) with $A_{568} = 0.5$ (solid line); action spectrum of the fast negative integrated displacement current amplitudes **A** (broken line); and action spectrum of the slow or final positive integrated displacement current amplitudes **B** (dotted line). The experimental errors in the **A** and **B** amplitudes are each ±10% of the **A** amplitudes, and the **A/B** data was measured at 2 nm intervals at 298 K.

subsequently refer to them as (time-resolved) integrated current amplitudes. We observed some variability in the ratio of the **B** amplitude (taken 500 μs after the laser flash) relative to the **A** amplitude (the instrument-limited response taken at approx. 5 μs after the flash) from sample to sample, but the **B** amplitude was usually more than 2-times larger than the **A** amplitude. The **B** amplitude can be correlated with the final charge displacement currents of protons inside the purple membranes. We then calculated the action spectra of the **A** and **B** integrated current amplitudes and compared them with the absorption spectrum of a light-adapted sample as shown in Fig. 4. Here, the **B** integrated current amplitudes have been normalized to the absorption spectrum maximum, and the A amplitudes had the same **A/B** amplitude ratio as that of the experimental time-resolved traces. Although the action spectrum of the **B** amplitudes is slightly red-shifted and weak in the $\lambda > 620$ nm region, there is a reasonable agreement with the optical absorption spectrum of BR. We can conclude that the final integrated charge displacements have an action spectrum closely resembling the absorption spectrum of light-adapted BR which indicates that the BR photochemical cycle is functioning in a nearly reversible manner in these sandwich cells.

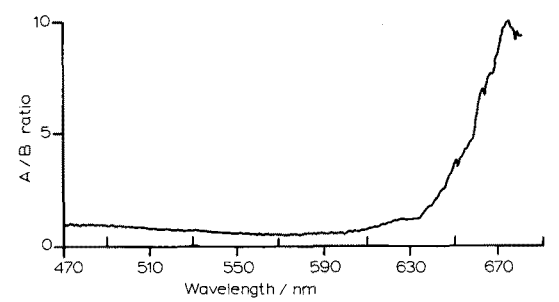

Fig. 5. Spectrum of the ratio of the **A/B** (fast over slow) integrated displacement current amplitudes from Fig. 4 which shows a red enhancement of the fast or negative integrated current amplitudes.

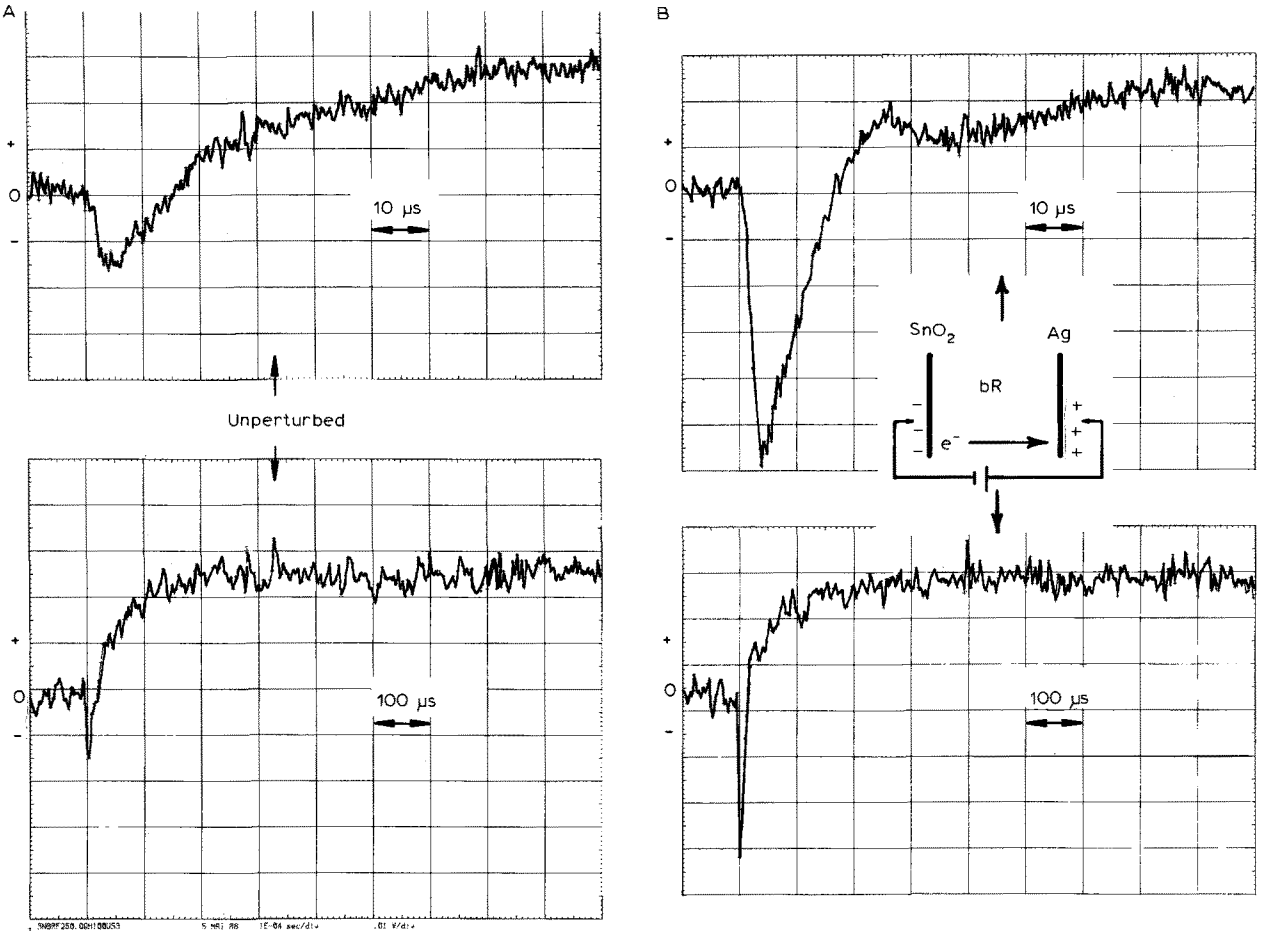

Fig. 6. (A) Time-resolved integrated displacement current amplitudes for a purple membrane sandwich cell at 298 K, measured under normal conditions with $A_{568} = 0.3$ and excited with a single 50 μJ laser flash at 570 nm. (B) Time-resolved integrated displacement current amplitudes measured for the same sandwich cell at 298 K excited with one laser flash at 570 nm, while applying 50 mV d.c. across the cell with the polarity indicated on the inset.

However, the instrument-limited **A** current amplitudes of Fig. 4 do not have an action spectrum comparable to that of the BR absorption spectrum. In addition, the ratio of the **A/B** integrated current amplitudes, shown in Fig. 5, varies as a function of the exciting wavelength. This sensitivity to excitation wavelength could suggest the presence of more than one light-absorbing species in these films, and we return to this question later in the conclusions.

Perturbed photocurrents

In order to provide more information concerning the nature of the charge carriers in this early time regime, we carried out a series of experiments where small d.c. currents were imposed upon the sandwich cells during the measurements of the flash-induced charge displacement currents. From our previous measurements of the impedance properties of our sandwich cells, we concluded that nanoampère d.c. electronic or ionic currents flowed through the cells upon application of small (20–100 mV) d.c. voltages across the external electrodes. We observed that the connection of the BR sandwich cell to an external d.c. power supply resulted in more noise being present during the measurement of the integrated charge displacement currents, but it was still possible to make single laser flash measurements with acceptable signal-to-noise ratios (see Fig. 6).

A strong effect on the measured integrated current amplitudes was observed when the polarity of the d.c. current was such that electrons or negative ions flowed from the SnO_2 electrode to the silver electrode, that is in the same direction as the transport of protons during the photochemical cycle of bacteriorhodopsin in these sandwich cells. As shown in Fig. 6, there was about a 3-fold enhancement of the early negative part of the charge displacement current with no appreciable increase in the integrated current amplitude observed at several 100 μs after flash excitation. Significantly, this enhancement effect was not observed in the case where the d.c. current polarity was reversed. Also, samples which had absorbances close to 0.5 were strongly perturbed on applying 50 mV acrosss the cells while samples with optical absorbances close to 1.0 were perturbed by applying 100 mV voltages. Increasing the

voltages past these thresholds resulted in increased noise, but it did not result in a further significant enhancement of the integrated charge displacement currents. Thus, the enhancement effect was already maximal at about 50 mV per 0.5 A unit. Using our calibration of the thickness of the cells, we determine that 0.5 in absorbance corresponds to a BR multilayer thickness of about 2.8 μm. Therefore, we can calculate that the electric field applied across the cells in these experiments is about $1.8 \cdot 10^4$ V/m, which is about 10^3-times smaller than the electric field used by Kononenko et al. [17] to perturb the spectra of purple membranes in the dark. Therefore, we conclude that it is very unlikely that the external electric field imposed on our cells was responsible for the perturbation effects observed in these experiments. This would imply that the d.c. currents or particularly the local electric fields associated with the currents were directly responsible for the perturbations observed in the time-resolved charge displacement currents. These latter currents can be as large as microampères/cm^2 [19], and yet they were apparently being perturbed by d.c. currents as small as nanoampères/cm^2. This could be explained if the role of the d.c. currents were to displace charges in the pores of the BR protein such that the photochemistry was triggered in pores which have become polarized. The major effect was observed at the instrument limited rise time of the negative integrated photocurrent maximum. Significantly, the amplitudes of the final integrated charge displacement currents were not affected as shown in Fig. 6. Therefore, we assume that the final proton charge displacement current was unaffected; but the charge carriers preceding the protons were influenced by the small applied potentials and concomitant nanoampère d.c. currents. We cannot make a direct comparison with the currents measured under voltage-clamp conditions which are essentially closed-circuit measurements made on membranes with aqueous interfaces, but these latter measurements [30] show some voltage asymmetry for the light-driven steady-state membrane currents in planar bilayer membranes. In contrast, we observe no voltage asymmetry for the final 'steady-state' proton displacement currents, which is probably due to the small value of our applied potentials reduced to those across single purple membrane bilayers.

It is well established that calcium, magnesium, and chloride ions, among others, are bound [31] in the purple membrane fragments isolated from the high-salt medium, and measurements by elemental analysis [31] find 0.93 Ca^{2+} and 3.4 Mg^{2+} as the molar ratios per mole of pigment in well-washed purple membranes. Indeed, deionization or loss of calcium and magnesium ions from purple membranes results in 'blue' membranes which are found to be incapable of pumping protons [31]. Therefore, we consider that ionic currents

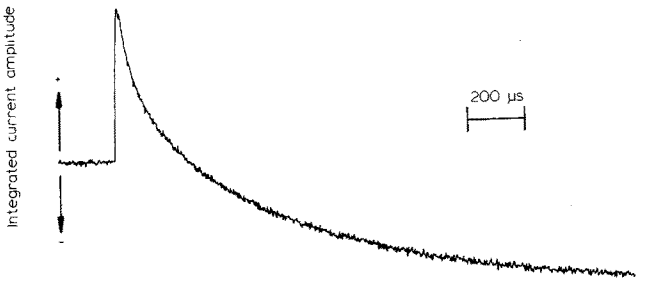

Fig. 7. Typical time-resolved integrated displacement current amplitude measured at 298 K for a sandwich cell with deionized blue membranes with a maximum optical absorption of $A_{605} = 0.4$, excited with a 50 μJ laser flash at 590 nm. The electrode polarity and ordinate sensitivity was the same as that of Fig. 3B, but the respective time scales were different as indicated on the respective figures.

were probably responsible for the small d.c. currents in our cells; but it seems unlikley that protons were mobile in these films, in the absence of photochemistry [32], firstly because of the buffering capacity of the groups in the protein and secondly because of the limited presence of water: only about 100 molecules of water per bacteriorhodopsin molecule at 50% relative humidity [13].

Finally, we produced some oriented solid films of deionized blue membranes from deposited purple membranes by electrodepositing at pH $\approx$ 6 and by passing the electrodeposition current through the deposited purple membranes for approx. 1–2 min. We show that deionized blue membranes do have a photochemical charge displacement activity, as shown in Fig. 7, where there is a positive amplitude followed by a small negative amplitude for charge displacements in the time profile. Here, the inverted character and much slower kinetics of the charge displacement currents (relative to those of purple membranes) together with the lack of a positive millisecond component are taken as evidence of an incomplete photochemical cycle, including a lack of proton pumping ability [31].

Conclusions

The measurement of charge displacement currents in the solid state cells has the advantage of eliminating the aqueous interface from considerations of the nature of the charge carriers implicated in the photochemical charge displacement mechanism. However, the kinetics of the major component of the M^{412} decay showed that the reversibility of the photochemical cycle was about two times slower than that observed for hydrated purple membranes. In spite of this slower decay, the photochemical yield of M^{412} was found to be comparable to that of the hydrated membrane reference. Therefore, we found no major deactivation of the dehydrated solid films; and their charge displacement currents possessed the expected bipolar (negative and positive) time pro-

file. However, we note that the 5% slow decay amplitude of the ΔA_{412} was probably indicative of some damage to the photocycle because this amplitude became much greater in samples where the electrodeposition times were much longer, that is, more than 15 s. In addition, the amplitude of the red shoulder was greater in the absorption spectra for these samples. In an extreme case, the membranes were deionized and blue, and their displacement currents were inverted and slower relative to those of purple membranes, as shown in Fig. 7.

On the basis of the previous discussion of the nature of the mobile charge carriers, involved in maintaining the nanoampère d.c. currents, it is clear that the candidates are electrons or more likely cations and/or anions. We consider the current of these charge carriers, not the small external electric field of only approx. 10^4 V/m, to be fully responsible for the perturbation of the charge displacement currents observed in Fig. 6. Upon applying d.c. currents with negative charges moving towards the exterior of the membrane, we observed an enhancement of the negative phase of the charge displacement current. We conclude that the migration of some mobile charge carriers are in fact affecting the negative phase of the photochemical charge displacement currents.

We postulate that mobile charge carriers such as unbound chloride ions could migrate through the pores of the protein towards the exterior of the membrane (or that alternatively unbound cations migrate in the opposite direction). The ionic current would create a local electric field which would tend to pull negative charges in the same direction as the negative current, that is towards the exterior of the membrane. Then during photochemical excitation, the splitting of the contact ion pairs could be enhanced by the presence of this local electric field created by the migration of negative charges away from the local environment towards the exterior side of the membrane. This concurs with the model (4), in which the negative counterion to the Schiff base (possibly Asp-212) is closer to the exterior side of the membrane than to the cytoplasmic side. Assuming that the negative phase of the charge displacement current is correlated with the splitting of the contact-ion pairs, this splitting could be enhanced by the current of negative carriers towards the outside of the membrane. Therefore, we concur with the generally accepted view of a two step mechanism overall: (1) photochemical dipole splitting followed by (2) proton pumping towards the exterior of the membrane.

It is significant that the final photochemically induced charge displacement currents had the same amplitudes in either the perturbed or unperturbed systems (see Fig. 6). This would imply that the application of the nanoampère d.c. currents perturbed only the initial phase of the charge displacement mechanism (the splitting of the contact ion pairs) and not the final proton displacements. This suggests that two kinds of current are being measured in the time-resolved charge displacements: (1) photochemically induced contact ion-pair splitting, perhaps involving Asp-212, in the early phase which can be perturbed by applying d.c. currents, and (2) photochemically displaced protons which cannot be perturbed by applying the same dc currents.

We now consider this interpretation with respect to the nature of the action spectra of Fig. 4, measured for the time resolved charge displacement amplitudes. The final amplitudes have an action spectrum which is in reasonable agreement with the absorption spectrum of BR in these solid films. However, the action spectrum of the early displacement current amplitudes does not agree with the BR absorption spectrum. The photochemical mechanism of dipole splitting and protein reorganization in the early time domain could give rise to the observed early action spectrum if there were some photostimulation of photointermediates absorbing in the red and blue wings of the BR absorption spectrum. On the basis of the measured optical decay of the M^{412} intermediate, its major decay time was 46 ms; but it did have a small ($\leqslant 5\%$) amplitude with a slower decay time of 0.97 ± 0.15 s. This could possibly suggest some trapping of the K, L, M, N and O photochemical intermediates as an alternative to the photocycle damage mechanism previously mentioned. However, we observed no significant spectral differences from the spectrum of light-adapted BR for samples which were repetitively pulsed at 0.2 Hz with dye laser pulses. Therefore, it is unlikely that M and other BR photocycle intermediates were trapped in significant amounts (e.g. $\geqslant 5\%$) in our solid state cells; and we note that the trapping of M is usually carried out at low temperatures under specific conditions [33].

However, we propose that there must be some trapping of red- and blue-absorbing intermediates to explain the form of the early action spectrum. One possibility is the trapping of small amounts of 'blue' membranes and their stable photoproduct, 'pink' membranes [34]. Particularly, we note the existence of the red sensitivity of Figs. 4 and 5, which suggests that several photochemically active species are present in these oriented membranes, albeit with small optical absorbances (according to the absorption spectra of Figs. 2 and 4). Also, the red shoulder of the solid film absorption spectra was enhanced upon prolonging the electrodeposition times. According to the result of Fig. 7, excitation of a small population of blue membranes would result in a different time-resolved charge displacement profile which is initially in the positive direction. However, we cannot explain the observed enhancement of the negative A amplitudes in the red wing of the action spectrum, based on our observation of a (completely opposite) positive initial current polarity

for the blue membranes. In addition, we observed that the small perturbing voltages, with the correct polarity, consistently resulted in stronger **A** photocurrent amplitudes for all photoexcitation wavelengths in the region between 470 nm and 670 nm for purple membrane samples with absorption spectra similar to that of Fig. 2. This suggests that the voltage sensitivity of the **A/B** ratios in these oriented purple membrane films is a property of photochemical centers of the purple membranes which absorb light between 470 nm and 670 nm.

However, it seems probable that other, yet to be discovered, trapped intermediates in these films are responsible for the nature of the early action spectrum (measured at 5 μs after excitation) which is correlated with the dipole splitting mechanism. These trapped intermediates would have their optical absorption in the blue and red wings of the action spectrum, and their photochemical activities would result in a negative initial photocurrent; but would not result in a significant proton pumping activity. However, the later action spectrum (measured at 500 μs after excitation) represents the reversible fraction of photochemical centers which can form M^{412} and participate in some proton pumping, albeit probably limited to the bilayer [17].

It is significant that the negative current amplitudes of Fig. 6 can be increased substantially by imposing nanoampère currents on the cells. This observation suggests that there is some inhibition of the observed dipole splitting component of the photocurrents and that this inhibition can be partially removed. It is known [1,35] that several backreactions occur between the photo intermediates and BR^{568}, particularly from the K intermediate, close to the primary photochemistry which has a quantum yield of 0.6 or more [35]. It is most probable that this latter back-reaction is being modulated in certain BR molecules by the applied d.c. currents so that we observe an enhanced dipole splitting yield with our microsecond time resolution. However, we note that these activated photochemical centers only exhibit negative polarity photocurrents and that they do not result in any increase in the proton pumping as measured in the late action spectrum as shown in Fig. 4. Another possibility which should be considered here is the proposal [35] that there are two kinds of light-adapted bacteriorhodopsin: those with a primary quantum yield of approx. 0.27 and those having a slightly displaced counterion with a primary quantum yield of approx. 0.74. It is possible that the back reaction from the K intermediate in these two populations of reaction centers could be modulated differentially. Therefore, we propose that the presence of two kinds of photochemical center could explain the existence of perturbable displacement currents and the apparent nonequivalence between the early action spectrum and the absorption spectrum in the oriented films of BR.

The mechanism of the photochemical cycle in these solid films is important because solid films of oriented purple membranes have been employed routinely in various spectroscopic measurements including the recent measurements of the orientation of the retinylidene pigment in the purple membrane [3,4]. A recent study of structural details revealed by neutron diffraction [33] also employed thin films of purple membranes. We conclude that there is only a small inhibition ($\leqslant 5\%$) of the photocycle in our electrodeposited solid films as compared with that of aqueous purple membrane suspensions. Thus, it is still possible to study the majority of reversibly active photochemical centers, albeit in the presence of some photochemical centers which only have negative photocurrents. Therefore, we suggest that it is important to measure ΔA_{412} in solid state films of purple membranes in order to characterize their photochemical efficiencies with respect to the formation of the M^{412} intermediate relative to that of purple membrane samples in aqueous suspensions at pH 7.

Acknowledgements

This research was supported by individual operating grants to A.R.M. and F.B. from the Natural Sciences and Engineering Research Council of Canada. We thank our colleagues Professor Roger M. Leblanc and Dr. S. Hotchandani for kindly permitting us to use the nitrogen-laser pumped dye laser and the electrical a.c. impedance equipment. We also wish to thank Mr. Thierry Lebihan and Mr. Normand Beaudoin, respectively, for technical assistance with the electrical and optical measurements.

References

1 Stoeckenius, W. and Bogomolni, R.A. (1982) Annu. Rev. Biochem. 52, 587–616.
2 Hofrichter, J., Henry, E.R. and Lozier R.H. 1989 Biophys. J. 56, 693–706.
3 Huang, J.Y. and Lewis, A. (1989) Biophys. J. 55, 835–842.
4 Lin, S.W. and Mathies, R.A. (1989) Biophys. J. 56, 653–660.
5 Braiman, M.S., Mogi, S.T., Marti, T., Stern, L.J., Khorana, H.G., Rothschild, K.J. (1988) Biochemistry 27, 8516–8520.
6 Fodor, S.P.A., Ames, J.B., Gebhard, R., Van den Berg, E.M.M., Stoeckenius, W., Lugtenberg, J. and Mathies, R.A. (1988) Biochemistry. 27, 7097–7101.
7 Keszthelyi, L. and Ormos, P. (1980) FEBS Lett. 109, 189–193.
8 Keszthelyi, L. and Ormos, P. (1983) Biophys. Chem. 18, 397–405.
9 Trissl, H.W. (1983) Biochim. Biophys. Acta 723, 327–331.
10 Trissl, H.W. and Montal, M. (1977) Nature 266, 655–657.
11 Varo, G. (1981) Acta biol. Acad. Sci. hung. 32, 301–310.
12 Groma, G.I., Szabo, G. and Varo, G. (1984) Nature 308, 557–558.
13 Varo, G. and Keszthelyi, L. (1983) Biophys. J. 43, 47–51.
14 Groma, G.I., Raksi, F., Szabo, G. and Varo, G. (1988) Biophys. J. 54, 77–80.
15 Chamorovskii, S.K., Kononenko, A.A., Rubin, A.B. and Chernavskii, D.S. (1987) Biofizika 32, 601–605.
16 Chamorovskii, S.K., Pikulenko, A.Y., Maksimychev, A.V., Lukashev, E.P., Pashchenko, V.Z., Kononenko, A.A. and Rubin, A.B. (1984) Dokl. Akad. Nauk SSSR 274, 738–741.

17 Kononenko, A.A., Lukashev, E.P., Maximychev, A.V., Chamorovsky, S.K., Rubin, A.B., Timashev, S.F. and Chekulaeva, L.N. (1986) Biochim. Biohys. Acta 850, 162–169.
18 Kononenko, A.A., Lukashev, E.P., Chamorovsky, S.K., Maximychev, A.V., Timashev, S.F., Chekulaeva, L.N., Rubin, A.B. and Paschenko, V.Z. (1987) Biochim. Biophys. Acta 892, 56–67.
19 Liu, S.Y. and Ebrey, T.G. (1988) Biophys. J. 54, 321–329.
20 Butt, H.J., Fendler, K., Bamberg, E., Tittor, J. and Oesterhelt, D. (1989) EMBO J. 8, 1657–1663.
21 Furuno, T., Takimoto, K., Kouyama, T., Ikegami, A. and Sasabe, H. (1988) Thin Solid Films 160, 145–151.
22 Warshel, A. and Barboy, N. (1982) J. Am. Chem. Soc. 104, 1469–1476.
23 Sandorfy, C. and Vocelle, D. (1986) Can. J. Chem. 64, 2251–2266.
24 Rothschild, K.J., Roepe, P., Lugtenburg, J., and Pardoen, J.A. (1984) Biochemistry 23, 6103–6109.
25 Okajima, T.L. and Hong, F.T. (1986) Biophys. J. 50, 901–912.
26 Ormos, P., Dancshazy, Z., and Keszthelyi, L. (1980) Biophys. J. 31, 207–214.
27 Kates, M., Kushwaha, S.C. and Sprott, G.D. (1982) Methods Enzymol. 88, 98–111.
28 Lozier, R.H., Bogomolni, R.A. and Stoeckenius, W. (1975) Biophys. J. 15, 955–962.
29 Ottolenghi, M., Rosenbach, V., Sheves, M., Baasov, T. and Friedman, N. (1983) in Photochemistry and Photobiology (Zewail, A.H., ed.), Vol. 2, pp. 829–855, Harwood, New York.
30 Braun, D., Dencher, N.A., Fahr, A., Lindau, M. and Heyn, M.P. (1988) Biophys. J. 53, 617–621.
31 Chang, C.-H., Chen, J.G., Govindjee, R. and Ebrey, T. (1985) Proc. Natl. Acad. Sci. USA 82, 396–400.
32 Srivastava, R.C. and Tandon, A. (1988) Biotech. Bioeng. 31, 511–515.
33 Dencher, N.A., Dresselhaus, D., Zaccai, G. and Buldt, G. (1989) Proc. Natl. Acad. Sci. USA. 86, 7876–7879.
34 Chang, C.H., Liu, S.Y., Jonas, R. and Govindjee, R. (1987) Biophys. J. 52, 617–623.
35 Birge, R.R., Cooper, T.M., Lawrence, A.F., Masthay, M.B., Vasilakis, C., Zhang, C.-F. and Zidovetzki, R. (1989) J. Am. Chem. Soc. 111, 4063–4074.